Journal of Computational Applied Mechanics 2024, 55(4): 771-782

DOI: 10.22059/jcamech.2024.382149.1220

RESEARCH PAPER

Investigating Heat-Induced Phase Transitions in POPC Lipid Bilayers Using Molecular Dynamics Simulations

Azadeh Kordzadeh [a], Saeed Javdansirat [b,*], Nasrin Javdansirat [b], Haibin Tang [c, d], Sajad Ghaderi [b], Amin Hadi [b, **], Reza Mahmoudi [b], Mohsen Nikseresht [b]

[a] *Chemical and Petroleum Engineering Department, Sharif University of Technology, Tehran, Iran*
[b] *Cellular and Molecular Research Center, Yasuj University of Medical Sciences, Yasuj, Iran*
[c] *Key Laboratory of Materials Physics, and Anhui Key Laboratory of Nanomaterials and Nanotechnology, Institute of Solid State Physics, HFIPS, Chinese Academy of Sciences, Hefei, Anhui 230031, China*
[d] *University of Science and Technology of China, Hefei, Anhui 230026, China*

Abstract

In this study, the effect of heat shock on the cell membrane was investigated using molecular dynamics (MD) simulations. Specifically, we examined the structural and dynamic behavior of a 1-palmitoyl-2-oleoyl-sn-glycero-3-phosphocholine (POPC) lipid bilayer as it was exposed to increasing temperatures ranging from 310K to 340K. The results revealed a significant transition in membrane behavior as temperature increased, particularly at 330K and 340K, where the bilayer exhibited characteristics of a fluid disordered phase. This transition was marked by an increase in the area per lipid, a decrease in bilayer thickness, and a reduction in the deuterium order parameter (Scd), indicating increased molecular disorder and membrane fluidity. Additionally, the number of hydrogen bonds between lipid head groups and surrounding water molecules declined, weakening electrostatic interactions and promoting bilayer permeability. At 330K and 340K, these changes contributed to the formation of transient pores, which could facilitate molecular transport across the bilayer. The optimal temperature for maintaining membrane stability while enhancing molecular diffusion was found to be 320K, where the bilayer retained an ordered structure and displayed increased lipid mobility without significant disruption. These findings provide valuable insights into the thermal regulation of membrane behavior, which has critical implications for processes such as drug delivery, gene transfection, and thermal therapy. Molecular dynamics simulations at the atomistic level allow us to uncover intricate details of membrane phase transitions that are challenging to observe experimentally.

Keywords: Molecular dynamics, Phospholipid bilayer, Heat shock, Gene transfection, Membrane permeability, Fluid disordered phase.

1. Introduction

Many studies have been conducted on physicochemical properties of lipid bilayers which are the first barrier to enter the cell and have a vital role in membrane function. Gene transfection is a powerful therapy for cancer and infection

*Corresponding authors: Saeed Javdansirat, Assistance Professor, javdansirat@gmail.com
**Amin Hadi, Assistance Professor, E-mail: s.amin.hadi@gmail.com, Amin.hadi@yums.ac.ir

diseases. There are different procedures including physical and chemical methods for gene transfection [1]. Physical gene transfection methods are electroporation [2, 3], sonoporation [4-6] and mechanoporation [7, 8]. In all of these methods, an external physical field into the cell causes cell membrane instability and the formation of pores in the cell. One of the methods investigated by the researchers for gene transfection is applying heat into the living cell. Takai et al. [9] showed that transfection and gene expression were enhanced with increasing temperature. Other studies indicated that transfection efficiency was increased during sonication [10, 11], as well as other methods such as electroporation [12] and polymer-mediated DNA delivery [13] by increasing temperature. Silva et al. [14] measured the electrical charge of the lipoplex surface by increasing temperature. They reported that increasing the incubation temperature from 25 to 50 °C resulted in positive charge re-localization in lipoplex surface (higher positive-potential) and higher lipoplex compaction (mean diameter reduction).

Different environmental conditions such as temperature, stretching, and chemical composition affect lipid bilayer behavior. It is demonstrated that the concentration of cholesterol has a condensing and ordering effect on lipid bilayer [15, 16]. Mukhpadhyay et al. [17] simulated the effect of NaCl solution on lipid bilayer properties. Their result exhibited that Na^+ ions penetrate deep into the ester region of the water lipid interface and ions do not have a significant effect on area per lipid and order parameter of the lipid bilayer.

Clarification of the temperature effect on the lipid bilayer and its transport behavior in the heat shock process is necessary. Lipid bilayers could have different phases that are temperature dependent, namely gel phase, liquid crystalline phase, subgel phase, and ripple phase. It is revealed that biological actions take place in the liquid crystalline phase therefore many studies have focused on recognizing physicochemical and mechanical properties of this phase [18, 19]. Garcia et al. [20] investigated the structure and phase transition of a lipid bilayer with atomic force microscopy (AFM). They observed a jump in force during the phase transition from the gel phase to the liquid crystalline phase. These results are experimentally in the macromolecular scale that are controlled by molecular interactions. Molecular dynamics (MD) simulation is a powerful method that can analyze the interaction between molecules in a system in atomistic level and reveals issues that are not observable experimentally [21].

In this study, the effect of increasing temperature on phospholipid bilayer membranes was investigated by MD simulation.

2. Simulation method

GROMACS 5.1.4 MD simulation package was used for employing MD simulation [22]. All-atom GROMOS54A7 force field [23] was used in all simulations with the simple point charge (SPC) model for water molecules [24]. Previous researches show that this force field is suitable for biomolecules [25-27]. The force field parameters for the lipid were taken from Ref. [28]. The temperature was kept constant by using V-rescale Thermostat and with a coupling time constant of 0.5 ps [29]. The pressure was maintained at 1 bar by applying the Berendsen algorithm with adjusting 2 ps for the coupling time constant [30]. The leap-frog algorithm was employed for integration of equations of motions under periodic boundary conditions in all directions with a time step of 1 fs. All bonds in each molecule including lipid and water were constrained by applying the linear constraint solver algorithm (LINCS) [31]. The Lennard-Jones cutoff radius was set to 1.2 nm. The electrostatic interactions were calculated by particle-mesh Evald (PME) [32] summation and the neighbor was updated by searching every 10 ps.

As it is illustrated in Fig.1 the 1-palmitoyl-2-oleoyl-sn-glycero-3-phosphocholine (POPC) was selected for simulation lipid bilayer [33-36]. A 128 POPC lipid bilayer with 64 lipids in each leaflet was placed in simulation box and solvated by 2460 water molecules. For all systems, the simulation box dimensions were (6.2 6.5 6.7) nm^3. This system was simulated at 310, 320,330, and 340 K. All simulations were performed in liquid crystalline phase [37]. After ensuring that the simulation cell has achieved equilibration, by energy minimization, the temperature was kept constant in the NVT ensemble for 10 ns, and then pressure and density were kept constant in NPT ensemble for 10 ns. The data collection was done in a NPT ensemble that its duration was 100 ns. This procedure and simulation times were the same as used in similar works [15, 16, 38-41] The visual molecular dynamics (VMD 1.9.1) program was used for molecular visualization [42].

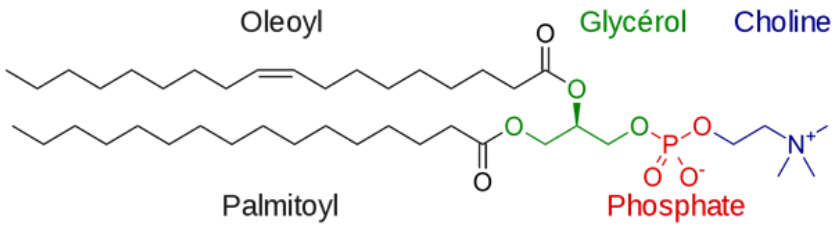

Fig. 1. Molecular structure of POPC lipid.

3. Results and discussion

3.1. Ensuring the equilibrium

The root mean square displacements (RMSD) is a suitable parameter to evaluate the equilibrium in simulated system. The RMSD of lipid molecules in each system is shown in Fig. 2. Systems have reached their equilibrium state after 20 ns of simulation time when the fluctuations in RMSDs have reduced significantly. Therefore, the MD trajectories extracted from the last 50 ns were used for further analysis [21].

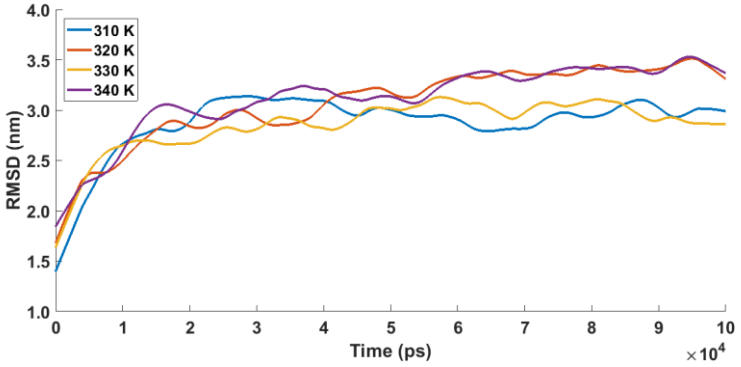

Fig. 2. RMSD plot of POPC at 310, 320, and 340 K versus simulation time.

3.2. Area per lipid

Packing of lipid molecules in a lipid bilayer could be described with area per lipid parameter. The average areas per lipid and thickness of bilayer in our simulations obtained by using the GridMat tool [43] are represented in Table 1 which are fairly close to the obtained values in the X-ray diffraction experiment, 65.8 nm^2, and 3.73 nm, respectively [37, 44]. By increasing temperature from 310 to 340 K the thickness of bilayer decreased by 1.422 Å. The time evolution of the area per lipid for the systems in each temperature is shown in Fig. 3. The area per lipid could be a suitable criterion for evaluating the equilibration and the stability of bilayer simulation. No significant fluctuations are observers in Fig. 3 justifies the equilibration of the simulation systems. By increasing temperature from 310K to 340 K the area per lipid has increased which is clearly shown in Fig. 4 and Fig. 5. It is necessary to mention that the obtained results are valid within the range of performed simulation time which is 100 ns. This simulation time is in accordance with previous studies [25-27, 39-41, 45, 46] and also RMSD and area per lipid (Fig.2 and Fig. 3) elucidated that these results obtained from equilibrated systems.

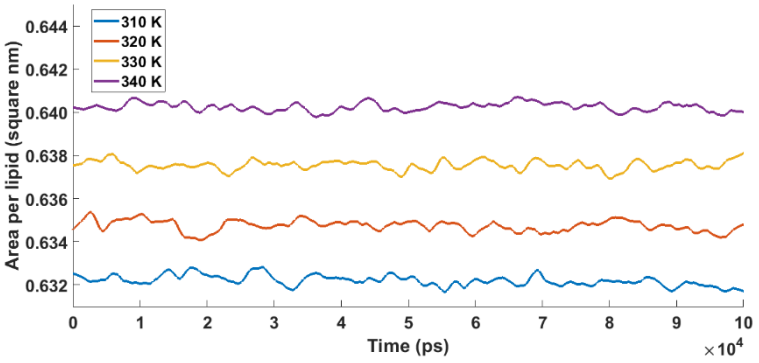

Fig. 3. The time evolution of the area per POPC lipid for the simulated systems.

Table 1. The average area per POPC lipid (A), the average thickness (h) of the POPC bilayer and the lateral diffusion coefficient of bilayer (D_{lipid}) and water molecules (D_{water}) at four temperatures.

Temperature (K)	A (nm^2)	h (nm)	D_{lipid}(10^5 cm^2/s)	D_{water}(10^5 cm^2/s)
310	0.6322	3.7975	0.004354	1.1211
320	0.6348	3.7859	0.008726	1.8188
330	0.6375	3.7676	0.017800	2.1010
340	0.6401	3.6553	0.028340	2.5683

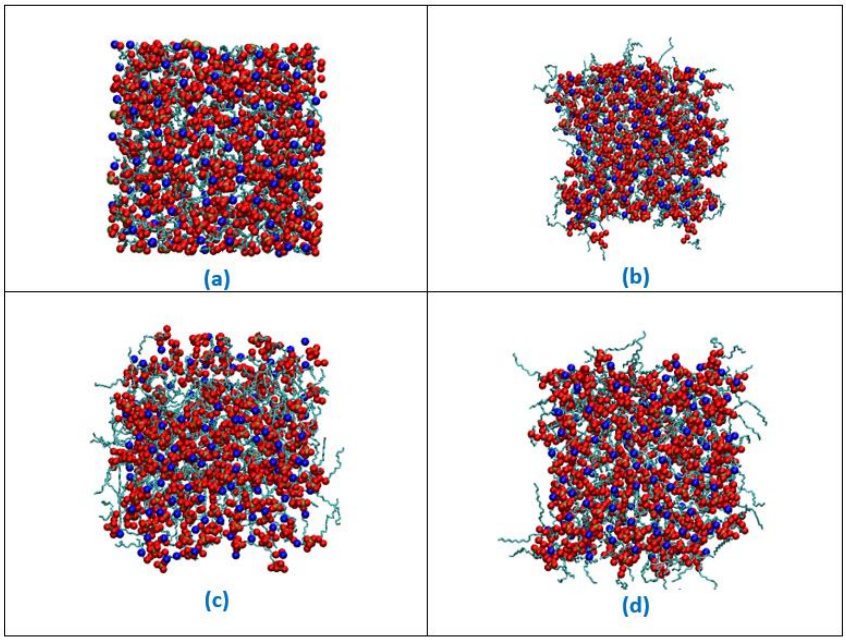

Fig. 4. Top view of POPC lipid bilayer after simulation at (a)310 K, (b) 320 K, (c) 330 K and (d)340 K. Oxygen, nitrogen and phosphorus atoms are shown in red, blue and yellow van der Waals spheres, respectively. Hydrophobic chains are shown with cyan lines. The water molecules were ignored for clarification. Videos S1, S2, S3, S4 and S5 in Supplementary Information shows simulation at 310, 320, 330 and 340 K respectively.

3.3. Order parameter

The ordering of hydrocarbon tails in bilayer is usually measured experimentally by the NMR spectroscopy, which can be quantified using deuterium order parameter S_{cd}. The deuterium order parameter S_{cd} in computer simulation is defined as equation (1):

$$S_{cd} = \langle \frac{3}{2} (\cos\theta)^2 - \frac{1}{2} \rangle \quad (1)$$

Where θ is the angle between the carbon-deuterium (CD) bond and the bilayer normal (z-axis), and the angular bracket denotes an ensemble average over time and all CD bonds. The effect of temperature on ordering the chain 1 (sn-1) and chain 2 (sn-2) of hydrophobic tail of POPC is presented in Fig. 6. By increasing temperature, the area per lipid has increased and lipids have more space for movement so the order parameter has decreased that this result is similar with previous theoretical studies [15, 16]. Also Seeling et al. [47, 48] derived an empirical equation from NMR spectroscopy that reveals the order parameter is inversely related to temperature which could describe our results in Fig. 6.

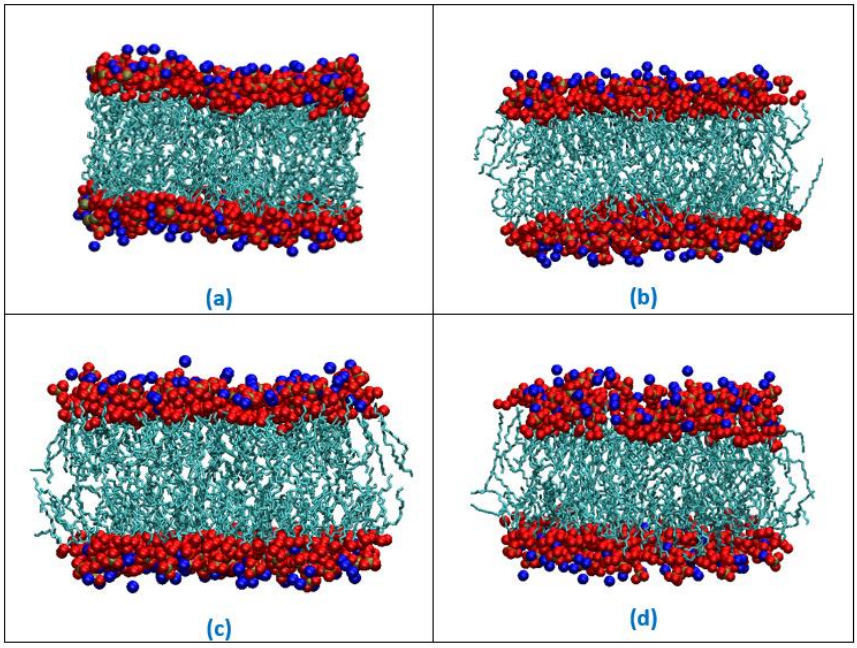

Fig. 5. Side view of POPC lipid bilayer after simulation at (a)310 K, (b) 320 K, (c) 330 K and (d)340 K. Oxygen, nitrogen and phosphorus atoms are shown in red, blue and yellow van der Waals spheres, respectively. Hydrophobic chains are shown with cyan lines. The water molecules were ignored for clarification.

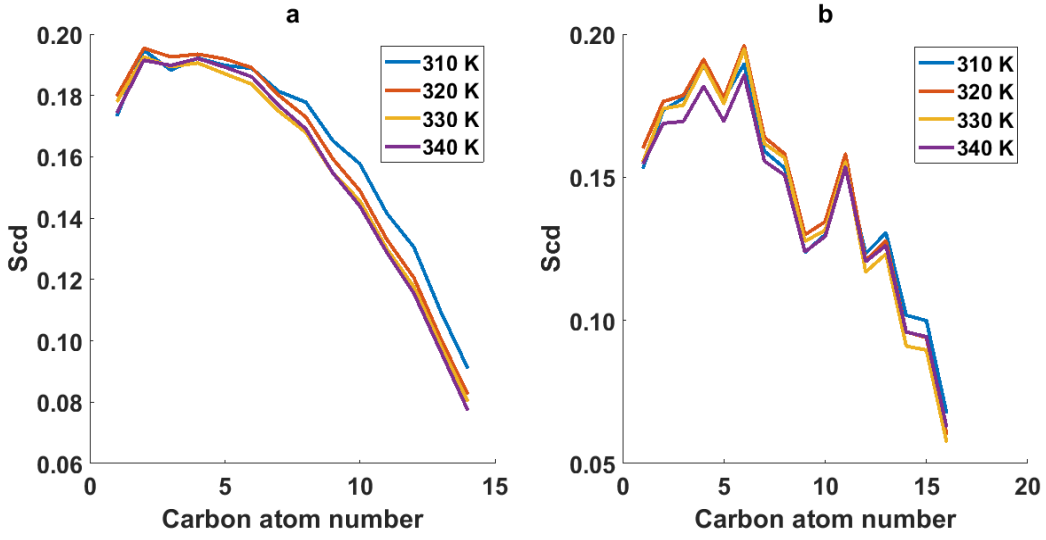

Fig. 6. Deuterium order parameter (S_{cd}) calculated for the (a) sn-1 and (b) sn-2 of the POPC lipid in the simulated systems.

3.4. Lateral diffusion coefficient

Mean square displacement (MSD) can be helpful in evaluating the lateral diffusion coefficient by using Einstein's equation (equation (2)):

$$D = \lim_{t \to \infty} \frac{1}{4} \frac{d}{dt} \langle [r(t + t_0) - r(t_0)]^2 \rangle_{t_0} \quad (2)$$

Where $r(t_0)$ and $r(t+t_0)$ are the position of the molecule at time t_0 and $t+t_0$, respectively. The angle bracket represents the mean square deviation at time t_0. MSDs of POPC lipids are depicted in Fig. 7, by increasing temperature the slope of MSD plots and so the diffusion coefficient have increased. Increasing area per lipid by increasing temperature facilitated transport of molecules across membrane and so the diffusion coefficient has increased according to Table 1 which are in agreement to previous studies [49]. Leib et al. [50, 51] suggested formation of pores enhances diffusion of molecules. Formation of pores at 330 and 340 K is obvious in Fig. 5.

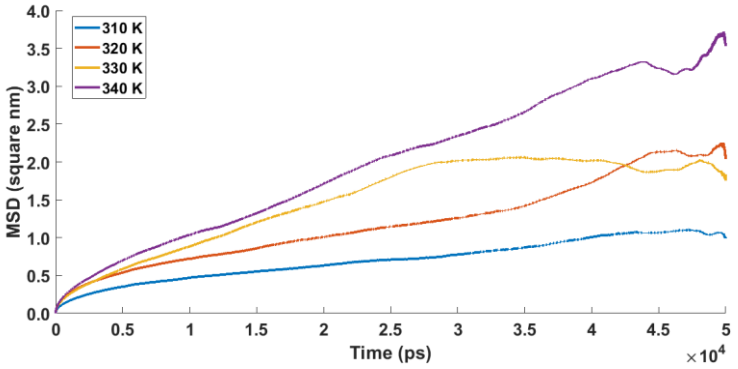

Fig. 7. MSD of POPC lipids in the simulated systems.

3.5. Mass density

As it is shown in Fig. 1 polar groups (head) of lipid orient towards intracellular and extracellular water and hydrophobic tails place in a position away from water and then a lipid bilayer forms. The density of head groups, tail groups, and water molecules are visualized in Fig. 8 (a), (b) and (c) respectively. The marked point in Fig. 8 (a) demonstrates that by increasing temperature from 310 to 340 K the density of head groups have decreased from 902 to 873 $\frac{kg}{m^3}$ and also the marked point at the center of lipid in Fig. 8 (b) exhibits that by elevation temperature from 310 to 340 K the density of tail groups have declined from 506 to 470 $\frac{kg}{m^3}$. The density reduction by rising temperature proves the formation of pores [50, 51], increase the area per lipid and decrease of the order parameter and the thickness of bilayer which is discussed in previous sections.

3.6. Movement of head groups

Table 2 shows that by increasing temperature from 310 to 340 K, the electrostatic interaction and the number of hydrogen bonds between head groups of lipid bilayer and water molecules have decreased. Also, the reduction of solvent accessible surface area (SASA) is the evidence of movement of polar groups. The scheme of solvent accessible surface area is shown in Fig. 9.

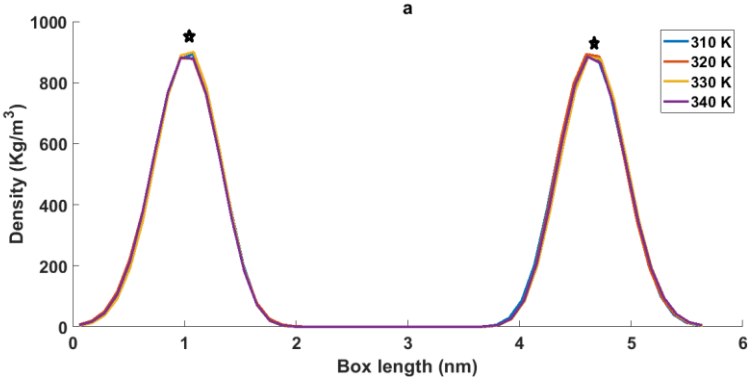

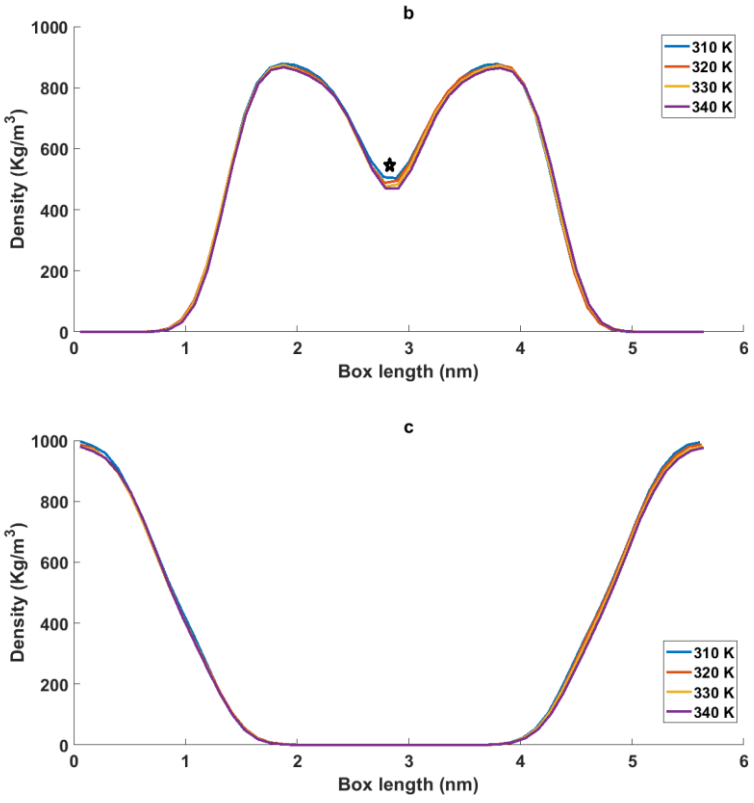

Fig. 8. The density profile of (a) head groups and (b) tail groups of POPC lipid and (c) water versus simulation box length for simulated systems.

By increasing temperature, the surface tension of lipid bilayer has declined (Table 2) which is in agreement with previous studies [52, 53].

The radial distribution function was used to examine the displacement of head groups. The radial probability of finding nitrogen atom from the center of mass (COM) of lipid bilayer is depicted in Fig. 10 (a). As it is illustrated in Fig.10 (a) at 310 and 320 K the nitrogen atoms have the same positions at radius of 2.59 nm from the COM of lipid bilayer. By increasing temperature to 330 and 340 the nitrogen atoms moved 1.10 and 3.30 Å towards hydrophobic tail, respectively. The radial probability of finding phosphorus atom from the COM of lipid bilayer is presented in Fig. 10 (b). As it is illustrated in Fig.10 (b) position of phosphorus atom is fix in 310 and 320 K and in 330 and 340 K phosphate group moved 1.00 Å towards hydrophobic part of lipid bilayer. This movement of poplar groups confirms the decrease in thickness of bilayer in section 4.2.

Garcia et al. [20] used AFM to investigate the effect of temperature on lipid bilayer. They observed a jump in force during gel to liquid crystalline phase transition that also was predictable by differential scanning calorimetry (DSC). When they continued increasing temperature, they observed a jump again in fore while no phase transition has occurred, they couldn't explain this observation. In this study, the POPC bilayer was simulated in liquid crystalline phase and our result elucidated this ambiguity in their experiment. By increasing temperature, the area per lipid has increased and therefore order parameter decreased. The radial probability proved that by increasing temperature the head groups moved and therefore the electrostatic interactions, the number of hydrogen bonds, and solvent accessible surface area were decreased. In real in 330 and 340 K a fluid disordered phase was occurred by displacement of choline and phosphate groups towards the interior of lipid bilayer.

4. Conclusion

In this study, the effect of temperature on lipid bilayer behavior and gene transfection efficiency were investigated by using molecular dynamics simulation. Garcia et al.[24] investigated effect of temperature on lipid bilayer by atomic force microscopy. They reported a jump in force at phase transition temperature that was predictable but this jump also observed in liquid crystalline phase that was ambiguous. In our study, an accurate molecular dynamics

simulation proved the formation of fluid disordered phase at 330 and 340 K by displacements of head groups that affects the electrostatic and physicochemical properties of bilayer. By increasing temperature from 310 to 320 K the area per lipid and diffusion coefficient of lipid bilayer increased while no significant disorder and movement observed in head groups. At 330 and 340 K choline and phosphate groups have a significant backward movement towards hydrophobic tail that formed a fluid disordered phase that is a kind of rupture [20]. As a result, the optimum temperature is 320 K in which the diffusion coefficient has increased and also the lipid bilayer has an ordered structure.

Table 2. The electrostatic interaction between head groups of lipid bilayer and water molecules (E), The solvent accessible surface area of head groups (SASA), the surface tension of lipid bilayer (δ) and number of hydrogen bonds between glycerol and phosphate groups of POPC and water molecules at four temperatures.

Temperature (K)	E(kJ/mol)	SASA (nm^2)	δ(bar.nm)	H-bond	
				Glycerol	Phosphate
310	-46747.6	323.61	193	324	460
320	-46705.0	322.25	166	319	457
330	-45241.5	321.33	104	315	455
340	-44521.9	320.61	95	308	448

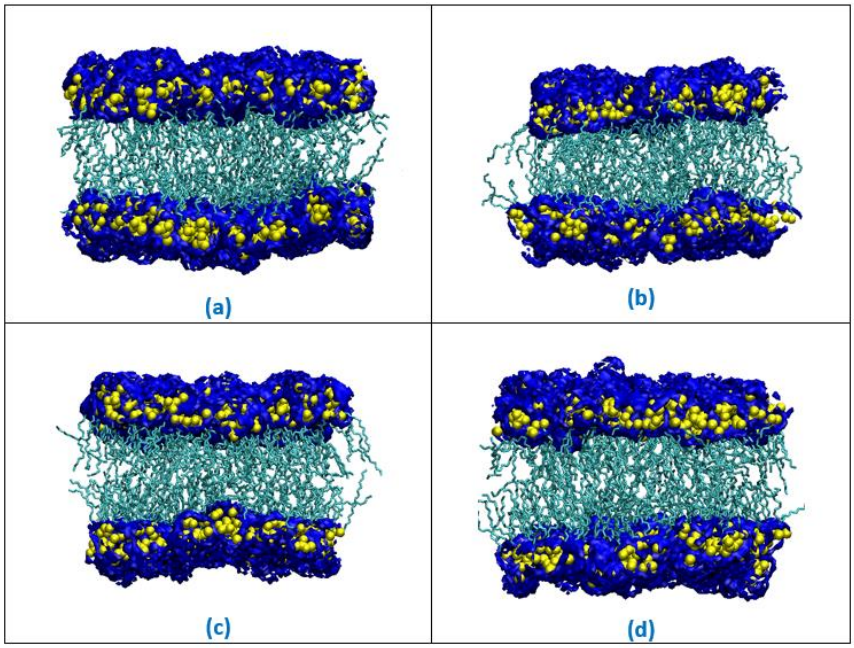

Fig. 9. Side view of solvent accessible surface area (SASA) of POPC lipid bilayer at (a)310 K, (b) 320 K, (c) 330 K and (d)340 K. head groups, hydrophobic chains and SASA are shown in yellow van der Waals spheres, cyan lines and blue surface, respectively. The water molecules were ignored for clarification.

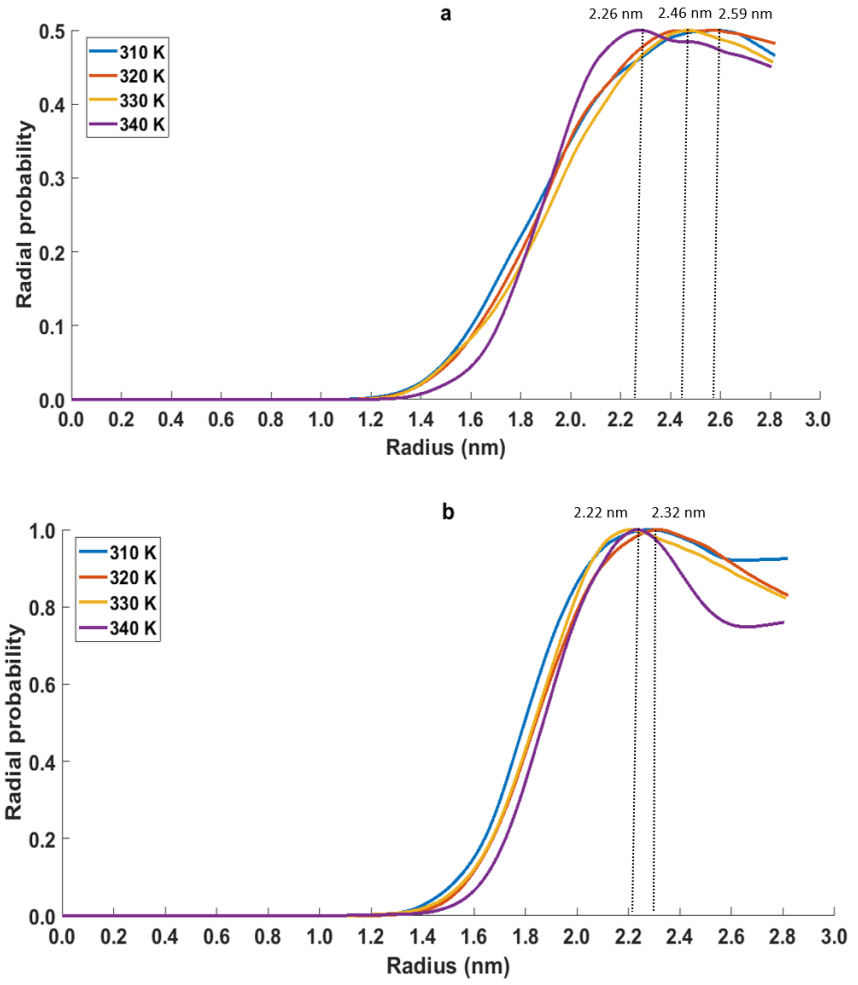

Fig. 10. The radial probability of (a) nitrogen and (b) phosphorus atom referenced to COM of lipid bilayer

5. Conflict of interest

There is no conflict of interest between authors.

References

[1] L. Salimzadeh, M. Jaberipour, A. Hosseini, A. Ghaderi, Non-viral transfection methods optimized for gene delivery to a lung cancer cell line, *Avicenna journal of medical biotechnology*, Vol. 5, No. 2, pp. 68, 2013.

[2] F. S. Barnes, B. Greenebaum, 2018, *Biological and medical aspects of electromagnetic fields*, CRC press,

[3] T. Kotnik, L. Rems, M. Tarek, D. Miklavčič, Membrane electroporation and electropermeabilization: mechanisms and models, *Annual review of biophysics*, Vol. 48, No. 1, pp. 63-91, 2019.

[4] A. Bouakaz, A. Zeghimi, A. A. Doinikov, Sonoporation: concept and mechanisms, *Therapeutic Ultrasound*, pp. 175-189, 2016.

[5] B. Helfield, X. Chen, S. C. Watkins, F. S. Villanueva, Biophysical insight into mechanisms of sonoporation, *Proceedings of the National Academy of Sciences*, Vol. 113, No. 36, pp. 9983-9988, 2016.

[6] N. Mignet, C. Marie, A. Delalande, S. Manta, M.-F. Bureau, G. Renault, D. Scherman, C. Pichon, Microbubbles for nucleic acid delivery in liver using mild sonoporation, *Nanotechnology for Nucleic Acid Delivery: Methods and Protocols*, pp. 377-387, 2019.

[7] M. P. Stewart, A. Sharei, X. Ding, G. Sahay, R. Langer, K. F. Jensen, In vitro and ex vivo strategies for intracellular delivery, *Nature*, Vol. 538, No. 7624, pp. 183-192, 2016.

[8] K. A. Hlavaty, M. G. Booty, S. Loughhead, K. Blagovic, A. Vicente-Suarez, D. Yarar, H. Bernstein, A. Sharei, Engineering a new generation of cell therapies for solid tumor oncology using the SQZ platform, *Cancer Research*, Vol. 79, No. 13_Supplement, pp. 3187-3187, 2019.

[9] T. Takai, H. Ohmori, Enhancement of DNA transfection efficiency by heat treatment of cultured mammalian cells, *Biochimica et Biophysica Acta (BBA)-Gene Structure and Expression*, Vol. 1129, No. 2, pp. 161-165, 1992.

[10] H. J. Kim, J. F. Greenleaf, R. R. Kinnick, J. T. Bronk, M. E. Bolander, Ultrasound-mediated transfection of mammalian cells, *Human gene therapy*, Vol. 7, No. 11, pp. 1339-1346, 1996.

[11] V. G. Zarnitsyn, M. R. Prausnitz, Physical parameters influencing optimization of ultrasound-mediated DNA transfection, *Ultrasound in medicine & biology*, Vol. 30, No. 4, pp. 527-538, 2004.

[12] M.-P. Rols, C. Delteil, G. Serin, J. Teissié, Temperature effects on electrotransfection of mammalian cells, *Nucleic acids research*, Vol. 22, No. 3, pp. 540, 1994.

[13] C. J. Frégeau, R. C. Bleackley, Factors influencing transient expression in cytotoxic T cells following DEAE dextran-mediated gene transfer, *Somatic cell and molecular genetics*, Vol. 17, No. 3, pp. 239-257, 1991.

[14] J. P. N. Silva, A. C. Oliveira, M. Lúcio, A. C. Gomes, P. J. Coutinho, M. E. C. R. Oliveira, Tunable pDNA/DODAB: MO lipoplexes: the effect of incubation temperature on pDNA/DODAB: MO lipoplexes structure and transfection efficiency, *Colloids and Surfaces B: Biointerfaces*, Vol. 121, pp. 371-379, 2014.

[15] A. Khajeh, H. Modarress, The influence of cholesterol on interactions and dynamics of ibuprofen in a lipid bilayer, *Biochimica et Biophysica Acta (BBA)-Biomembranes*, Vol. 1838, No. 10, pp. 2431-2438, 2014.

[16] A. Khajeh, H. Modarress, Effect of cholesterol on behavior of 5-fluorouracil (5-FU) in a DMPC lipid bilayer, a molecular dynamics study, *Biophysical chemistry*, Vol. 187, pp. 43-50, 2014.

[17] P. Mukhopadhyay, L. Monticelli, D. P. Tieleman, Molecular dynamics simulation of a palmitoyl-oleoyl phosphatidylserine bilayer with Na+ counterions and NaCl, *Biophysical journal*, Vol. 86, No. 3, pp. 1601-1609, 2004.

[18] J. F. Nagle, S. Tristram-Nagle, Structure of lipid bilayers, *Biochimica et Biophysica Acta (BBA)-Reviews on Biomembranes*, Vol. 1469, No. 3, pp. 159-195, 2000.

[19] J. F. Nagle, H. I. Petrache, N. Gouliaev, S. Tristram-Nagle, Y. Liu, R. M. Suter, K. Gawrisch, Multiple mechanisms for critical behavior in the biologically relevant phase of lecithin bilayers, *Physical Review E*, Vol. 58, No. 6, pp. 7769, 1998.

[20] S. Garcia-Manyes, G. Oncins, F. Sanz, Effect of temperature on the nanomechanics of lipid bilayers studied by force spectroscopy, *Biophysical journal*, Vol. 89, No. 6, pp. 4261-4274, 2005.

[21] A. Kordzadeh, S. Amjad-Iranagh, M. Zarif, H. Modarress, Adsorption and encapsulation of the drug doxorubicin on covalent functionalized carbon nanotubes: A scrutinized study by using molecular dynamics simulation and quantum mechanics calculation, *Journal of Molecular Graphics and Modelling*, Vol. 88, pp. 11-22, 2019.

[22] D. Van Der Spoel, E. Lindahl, B. Hess, G. Groenhof, A. E. Mark, H. J. Berendsen, GROMACS: fast, flexible, and free, *Journal of computational chemistry*, Vol. 26, No. 16, pp. 1701-1718, 2005.

[23] W. F. van Gunsteren, S. Billeter, A. Eising, P. Hünenberger, P. Krüger, A. Mark, W. Scott, I. Tironi, Biomolecular simulation: the GROMOS96 manual and user guide, *Vdf Hochschulverlag AG an der ETH Zürich, Zürich*, Vol. 86, pp. 1-1044, 1996.

[24] H. J. Berendsen, J. P. Postma, W. F. van Gunsteren, J. Hermans, Interaction models for water in relation to protein hydration, in *Proceeding of*, Springer, pp. 331-342.

[25] S. Amjad-Iranagh, A. Yousefpour, P. Haghighi, H. Modarress, Effects of protein binding on a lipid bilayer containing local anesthetic articaine, and the potential of mean force calculation: a molecular dynamics simulation approach, *Journal of molecular modeling*, Vol. 19, pp. 3831-3842, 2013.

[26] A. Yousefpour, H. Modarress, F. Goharpey, S. Amjad-Iranagh, Combination of anti-hypertensive drugs: a molecular dynamics simulation study, *Journal of Molecular Modeling*, Vol. 23, pp. 1-18, 2017.

[27] A. Yousefpour, H. Modarress, F. Goharpey, S. Amjad-Iranagh, Interaction of drugs amlodipine and paroxetine with the metabolizing enzyme CYP2B4: a molecular dynamics simulation study, *Journal of Molecular Modeling*, Vol. 24, pp. 1-11, 2018.

[28] O. Berger, O. Edholm, F. Jähnig, Molecular dynamics simulations of a fluid bilayer of dipalmitoylphosphatidylcholine at full hydration, constant pressure, and constant temperature, *Biophysical journal*, Vol. 72, No. 5, pp. 2002-2013, 1997.

[29] G. Bussi, D. Donadio, M. Parrinello, Canonical sampling through velocity rescaling, *The Journal of chemical physics*, Vol. 126, No. 1, 2007.

[30] H. J. Berendsen, J. v. Postma, W. F. Van Gunsteren, A. DiNola, J. R. Haak, Molecular dynamics with coupling to an external bath, *The Journal of chemical physics*, Vol. 81, No. 8, pp. 3684-3690, 1984.

[31] H.-d. Zheng, B.-y. Wang, Y.-x. Wu, Molecular dynamics simulation on the interfacial features of phenol extraction by TBP/dodecane in water, *Computational and Theoretical Chemistry*, Vol. 970, No. 1-3, pp. 66-72, 2011.

[32] T. Darden, D. York, L. Pedersen, Particle mesh Ewald: An N· log (N) method for Ewald sums in large systems, *The Journal of chemical physics*, Vol. 98, No. 12, pp. 10089-10092, 1993.

[33] B. Jójárt, T. A. Martinek, Performance of the general amber force field in modeling aqueous POPC membrane bilayers, *Journal of computational chemistry*, Vol. 28, No. 12, pp. 2051-2058, 2007.

[34] K. L. Koster, M. S. Webb, G. Bryant, D. V. Lynch, Interactions between soluble sugars and POPC (1-palmitoyl-2-oleoylphosphatidylcholine) during dehydration: vitrification of sugars alters the phase behavior of the phospholipid, *Biochimica et Biophysica Acta (BBA)-Biomembranes*, Vol. 1193, No. 1, pp. 143-150, 1994.

[35] M. Fidorra, L. Duelund, C. Leidy, A. C. Simonsen, L. Bagatolli, Absence of fluid-ordered/fluid-disordered phase coexistence in ceramide/POPC mixtures containing cholesterol, *Biophysical journal*, Vol. 90, No. 12, pp. 4437-4451, 2006.

[36] M. L. Frazier, J. R. Wright, A. Pokorny, P. F. Almeida, Investigation of domain formation in sphingomyelin/cholesterol/POPC mixtures by fluorescence resonance energy transfer and Monte Carlo simulations, *Biophysical journal*, Vol. 92, No. 7, pp. 2422-2433, 2007.

[37] D. P. Tieleman, L. R. Forrest, M. S. Sansom, H. J. Berendsen, Lipid properties and the orientation of aromatic residues in OmpF, influenza M2, and alamethicin systems: molecular dynamics simulations, *Biochemistry*, Vol. 37, No. 50, pp. 17554-17561, 1998.

[38] !!! INVALID CITATION !!! [42-44].

[39] A. Yousefpour, S. Amjad Iranagh, Y. Nademi, H. Modarress, Molecular dynamics simulation of nonsteroidal antiinflammatory drugs, naproxen and relafen, in a lipid bilayer membrane, *International Journal of Quantum Chemistry*, Vol. 113, No. 15, pp. 1919-1930, 2013.

[40] A. Yousefpour, S. Amjad-Iranagh, F. Goharpey, H. Modarress, Effect of drug amlodipine on the charged lipid bilayer cell membranes DMPS and DMPS+ DMPC: A molecular dynamics simulation study, *European Biophysics Journal*, Vol. 47, pp. 939-950, 2018.

[41] Y. Nademi, S. AMJAD IRANAGH, A. Yousefpour, S. Z. Mousavi, H. Modarress, Molecular dynamics simulations and free energy profile of Paracetamol in DPPC and DMPC lipid bilayers, *Journal of Chemical Sciences*, Vol. 126, pp. 637-647, 2014.

[42] W. Humphrey, A. Dalke, K. Schulten, VMD: visual molecular dynamics, *Journal of molecular graphics*, Vol. 14, No. 1, pp. 33-38, 1996.

[43] W. J. Allen, J. A. Lemkul, D. R. Bevan, GridMAT-MD: a grid-based membrane analysis tool for use with molecular dynamics, *Journal of computational chemistry*, Vol. 30, No. 12, pp. 1952-1958, 2009.

[44] X. Zhuang, J. R. Makover, W. Im, J. B. Klauda, A systematic molecular dynamics simulation study of temperature dependent bilayer structural properties, *Biochimica et Biophysica Acta (BBA)-Biomembranes*, Vol. 1838, No. 10, pp. 2520-2529, 2014.

[45] A. Yousefpour, H. Modarress, F. Goharpey, S. Amjad-Iranagh, Interaction of PEGylated anti-hypertensive drugs, amlodipine, atenolol and lisinopril with lipid bilayer membrane: A molecular dynamics simulation study, *Biochimica et Biophysica Acta (BBA)-Biomembranes*, Vol. 1848, No. 8, pp. 1687-1698, 2015.

[46] S. Singh, Dynamics of heroin molecule inside the lipid membrane: A molecular dynamics study, *Journal of Molecular Modeling*, Vol. 25, No. 5, pp. 121, 2019.

[47] J. Seelig, A. Seelig, Lipid conformation in model membranes and biological membranes, *Quarterly reviews of Biophysics*, Vol. 13, No. 1, pp. 19-61, 1980.

[48] A. Seelig, J. Seelig, Dynamic structure of fatty acyl chains in a phospholipid bilayer measured by deuterium magnetic resonance, *Biochemistry*, Vol. 13, No. 23, pp. 4839-4845, 1974.

[49] D. Bassolino-Klimas, H. E. Alper, T. R. Stouch, Mechanism of solute diffusion through lipid bilayer membranes by molecular dynamics simulation, *Journal of the American Chemical Society*, Vol. 117, No. 14, pp. 4118-4129, 1995.

[50] W. Lieb, W. Stein, *The molecular basis of simple diffusion within biological membranes*, in: *Current topics in membranes and transport*, Eds., pp. 1-39: Elsevier, 1972.

[51] W. Lieb, W. Stein, Biological membranes behave as non-porous polymeric sheets with respect to the diffusion of non-electrolytes, *Nature*, Vol. 224, No. 5216, 1969.

[52] S. Palmer, The effect of temperature on surface tension, *Physics Education*, Vol. 11, No. 2, pp. 119, 1976.

[53] H. Leontiadou, A. E. Mark, S. J. Marrink, Molecular dynamics simulations of hydrophilic pores in lipid bilayers, *Biophysical journal*, Vol. 86, No. 4, pp. 2156-2164, 2004.